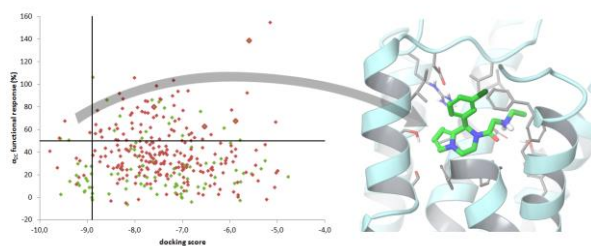## Graphical Abstract

Cell-based and virtual fragment screening for adrenergic α₂c receptor agonists

Leave this area blank for abstract info.

Edit Szőllősi, Amrita Bobok, László Kiss, Márton Vass, Dalma Kurkó, Sándor Kolok, András Visegrády, György M. Keserű

Gedeon Richter Plc., Gyömrői út 19-21. Budapest, H-1103, Hungary

Cell-based and virtual fragment screening for adrenergic α₂C receptor agonists

Edit Szőllősi[a], Amrita Bobok[a], László Kiss[a], Márton Vass[a], Dalma Kurkó[a], Sándor Kolok[a], András Visegrády[a], György M. Keserű[b,*]

[a] Gedeon Richter Plc., Gyömrői út 19-21. Budapest, H-1103, Hungary
[b] Research Centre for Natural Sciences of the Hungarian Academy of Sciences, Magyar tudósok körútja 2. Budapest, H-1117, Hungary

*Corresponding author (GMK) Phone: +36-1-382-6900 Fax: +36-1-382-6297 E-mail: gy.keseru@ttk.mta.hu

ARTICLE INFO

ABSTRACT

Fragment-based drug discovery has emerged as an alternative to conventional lead identification and optimization techniques generally supported by biophysical detection techniques. Membrane targets like G protein-coupled receptors (GPCRs), however, offer challenges in lack of generic immobilization or stabilization methods for the dynamic, membrane-bound supramolecular complexes. Also modeling of different functional states of GPCRs proved to be a challenging task. Here we report a functional cell-based high concentration screening campaign for the identification of adrenergic α₂C receptor agonists compared with the virtual screening of the same ligand set against an active-like homology model of the α₂C receptor. The conventional calcium mobilization-based assay identified active fragments with a similar incidence to several other reported fragment screens on GPCRs. 16 out of 3071 screened fragments turned out as specific ligands of α₂C, two of which were identified by virtual screening as well and several of the hits possessed surprisingly high affinity and ligand efficiency. Our results indicate that *in vitro* biological assays can be utilized in the fragment hit identification process for GPCR targets.

1. Introduction

Fragment-based lead discovery offers more efficient sampling of medicinal chemistry space and exploiting optimal interactions with the protein target that makes this approach increasingly popular.[1,2] Since emphasis is placed more on interaction efficiency rather than binding affinity per se, sensitive biophysical detection techniques including X-ray crystallography, NMR spectroscopy[3,4] and surface plasmon resonance,[5] but also thermal shift assays[6] and biochemical screening[7] are used in the primary screening phase of fragment-based drug discovery (FBDD) programs.

G protein-coupled receptors (GPCRs) form a significant portion of potential targets of novel drugs,[8] thus application of fragment screening to GPCRs is a well-founded objective. While for soluble targets numerous successful FBDD programs are documented,[1,9] reports on fragment screening for membrane proteins are much sparser. SPR was applied successfully using immobilized and tagged membrane proteins[10-12] while researchers from Heptares and ZoBio reported the use of target immobilized NMR screening (TINS) on thermostabilized GPCRs.[10,13] A novel adenosine A₃ receptor specific fluorescent label enabled development of a fluorescence intensity-based whole cell binding assay[14] capable of identifying low affinity ligands of A₃. Apart from these successful examples, where challenging target-specific preparations were crucial for the actual screening

process, some experiences with more generic assay formats for probing membrane proteins have been reported as well.[15-17]

Often, drug discovery programs require ligands that stimulate or potentiate membrane receptors. Although the understanding on the molecular basis of GPCR function increased tremendously in the last years,[18] the structural basis of distinct biological responses is still poorly understood. GPCR activation pathways have only recently been tackled by crystallographic[19] and molecular modeling[20,21] efforts. Cellular *in vitro* assays, where the molecular target is presented in a biologically relevant functional form, available at most screening laboratories, could be theoretically applied widely to identify ligands for membrane targets of different functional activity. Despite good availability, some concerns about these assays arise: assay interference caused by high test concentrations, sensitivity of functional assays and the lack of structural information. In this study our aim was to assess the utility of *in vitro* biological assays to fragment-based lead discovery for GPCR agonists and to explore hit validation strategies following fragment hit discovery and our findings on adrenergic α₂C receptor are reported.

The adrenergic α₂C receptor belongs to class A GPCRs and agonists selectively activating this receptor might offer therapeutic benefits in analgesia, anesthesia or various CNS indications.[22,23] The major limitation for development of α₂C receptor agonists has proven to be the high degree of similarity to

undesired homologues, especially α_{2A}, and discovery of sufficiently selective ligands has been found troublesome. We speculated that identifying novel molecular fragments efficiently binding to α_{2C} could provide sufficient room to improve subtype selectivity.

Moreover, as the structure of the adrenergic α_{2C} receptor binding site is not available yet, homology modeling was performed in order to do a head-to-head comparison of experimental and virtual agonist fragment screening and to provide binding hypotheses for the identified hit compounds. Although the activation process brings about little structural change in the binding site, it was shown that molecular docking of agonist ligands to activated structural models is preferred[24] and an agonist-bound homology model of the CB_2 receptor was successfully used in identifying novel agonists from virtual screening.[25] Activated structural models generated using molecular dynamics simulation were also shown to be capable of retrieving agonist ligands in retrospective virtual screening studies.[21,26]

2. Results and discussion

2.1. Experimental fragment screening

In preparation for a fragment screening for the identification of α_{2C} agonists, all options for screening assays were considered. In lack of a thermostabilized receptor variant and a validated immobilization technique for the target, radioligand displacement assay and functional assay utilizing a chimeric G protein[27] have been selected for further evaluation. 160 diverse compounds selected from the Maybridge Rule of Three core library have been tested in both assay formats at 250 µM concentration. While in the functional test only 3 compounds displayed agonistic activity above 50%, 48 compounds possessed activity above 50% in the displacement assay. This phenomenon was specific to α_{2C}, as radioligand displacement at an unrelated peptidergic receptor resulted in no actives from the same representative set of fragments. As we opted to assess the performance of a biological screening method in a generic setting, the unusually high hit rate in a binding test was taken with precaution and the functional calcium mobilization assay was chosen for hit identification.

3071 compounds fulfilling the fragment criteria were screened at 250 µM in duplicates in the cell-based functional assay. The screen was performed with an average Z' of 0.80 and average Z of 0.63, indicating low variability in assay.[28] An activity threshold of 50% resulted in 318 actives corresponding to 10.3% of screened compounds. Upon retesting these samples, 86 compounds gave higher than 50% response at 250 µM. This surprisingly low confirmation rate (27%) was presumably the result of the inter-day variability in the sensitivity of the cellular assay, as during confirmation most compounds (217 out of 318) surpassed the 50% activity threshold at 500 µM and the EC_{50} of reference agonist UK14,304 was also slightly right-shifted at retesting (data not shown).

To rule out nonspecific activity caused by the high screening concentration, all actives were tested for their agonistic like effect on sst_4 receptor expressing cells utilizing the same protocol as the α_{2C} assay. 21 of the 86 confirmed actives displayed less than 30% fluorescence response at the sst_4 receptor and 20 of them were pure samples as determined with HPLC/MS. To confirm target specific interaction, the resulting 20 samples underwent radioligand displacement assay on α_{2C}, where 16 compounds displayed concentration dependence for binding and at least 50% displacement at 500 µM. Interestingly, functional responses elicited by 3 of the remaining 4 compounds could be at

least partially inhibited by the orthosteric α_2 antagonist MK-912. Our fragment screening campaign thus led to the identification of 16 validated agonist fragment hits at the α_{2C} receptor.

Next, all hits were characterized for binding affinity, agonist potency and efficacy at the α_{2C} receptor utilizing the above assays. To assist evaluation of binding efficiency, ligand efficiency (LE) and ligand-efficiency-dependent lipophilicity (LELP) were derived from K_i values as described in the literature.[29,30] Table 1 demonstrates representative data for the validated hits. Numerous chemically diverse highly potent and efficient fragment hits were identified from this commercially available screening set. Interestingly, functional hit profiles showed a high degree of heterogeneity: low efficacy and high potency hits displaying partial agonism relative to UK14,304 in the calcium assay with equal affinity as full agonist of low potency were observed (e.g. compare effects of compounds **2** and **4** in Figure 1 and Table 1). Finally to assess novelty, chemical similarity to known α_{2C} receptor ligands from the ChEMBL bioactivity database was calculated and the most similar structures are shown in Table 1. Fragment **1** is a known alpha adrenergic agonist from the imidazoline family. Compound **4** is a known dopaminergic ligand, however, its adrenergic effect has not yet been reported. The rest of the fragments had moderately similar or no analogues among known α_{2C} ligands.

Screening fragments at high concentration in biological assays has its limitations, most notably higher risk of nonspecific effects observed, lower sensitivity and lack of structural information on binding. The fact that the hit rate for α_{2C} agonists in a functional assay was comparable to that of other screening approaches indicates that assay interference did not hinder screening in general in the biological setting. Although a significant portion of hits were discarded after counter-screening, it has to be noted that owing to potentially low specificity of fragment hits[17] straightforward counter-screening at an unrelated target could significantly overestimate non-specificity. Thus, orthogonal on-target assays confirming molecular mechanism of action should be preferred instead. Moreover, several in vitro assays are available less prone to nonspecific interference.[31,32] Sensitivity in the biological assay in contrast is expected to be inferior to those in biophysical formats, although the latter methods often also require demonstration of relevance of binding in a functional context. The limitation of reduced sensitivity can
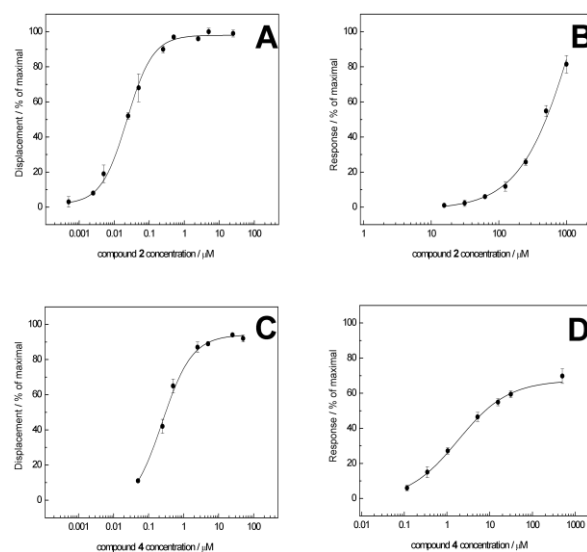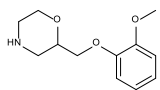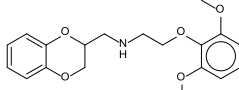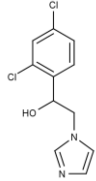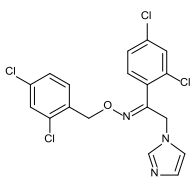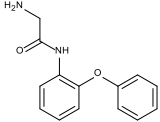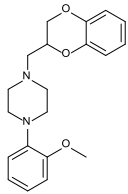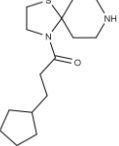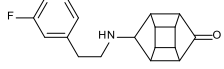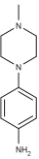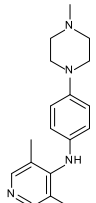

Figure 1. Diversity of binding and functional responses with fragment hits. Concentration response curves for compounds **2** and **4** in radioligand displacement (graphs *A* and *C*) and agonistic effect in calcium mobilization assay (graphs *B* and *D*) expressed as percentage of maximal effect.

Table 1. Pharmacological parameters of fragment hits.

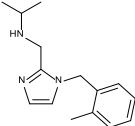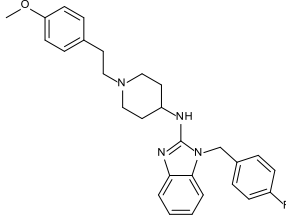| Cpd.	Structure	Radioligand displacement			Calcium mobilization			LE	LELP	Most similar compound in ChEMBL
		pKi		Emax / %	pEC50		Emax / %			
		mean	SD		mean	SD				
1		8.64	0.10	102	7.26	0.21	55	0.74	3.0	Naphazoline (exact)
2		7.93	0.02	100	<3.30	N.D.	>75	0.64	4.5	
3		7.14	0.17	100	6.76	0.24	60	0.70	2.1	
4		7.08	0.06	92	5.86	0.10	70	0.51	3.7	
5		6.27	0.05	92	<3.30	N.D.	>66	0.57	4.3	
6		6.19	0.12	92	5.50	0.39	49	0.65	2.4	
7		5.97	0.15	98	5.46	0.15	56	0.41	5.9	
8		5.93	0.01	97	<3.30	N.D.	>105	0.62	4.1	
9		5.28	0.10	102	3.32	0.11	87	0.36	5.6	
10		5.14	0.04	99	<3.30	N.D.	>88	0.32	7.7	
11		5.08	0.06	104	<3.30	N.D.	>51	0.36	6.0	

12		4.98	0.06	81	<3.30	N.D.	>77	0.42	2.7
13		4.82	0.10	78	3.47	0.17	123	0.41	5.8
14		4.81	0.09	81	3.20	0.12	93	0.36	4.9
15		4.81	0.18	81	<3.3	N.D.	>82	0.35	7.5
16		4.65	0.07	102	3.83	0.06	55	0.35	7.7
17[a]		5.82	N.D.	100	<3.3	N.D.	>36	0.57	1.9

[a]The only hit from the MayBridge validation library with sst$_4$ response <10% at 250 μM.

N.D. Not determined

be compensated by screening compounds of slightly higher complexity than those in X-ray or NMR studies,[33] as the higher throughput of established plate-based biological assays enables screening of larger compound libraries. These libraries still sample chemical space more efficiently than conventional HTS collections while they are expected to produce higher affinity ligands than less complex libraries.[34] Lastly, lack of structural information is definitely a shortcoming of biological fragment screening and it is yet to be demonstrated that efficient fragment optimization and evolution is possible on GPCR targets with either biophysical or biological methods.

2.2. Virtual fragment screening

The homology model of the activated α$_{2C}$ receptor was constructed using the human adrenergic β$_2$ X-ray structure crystallized with a nanobody stabilizing the active state as template. The binding site was optimized using known agonists of the α$_{2C}$ receptor in the Schrödinger Induced Fit Docking protocol. The best structure for virtual screening was selected based on retrospective enrichment studies over a ligand set of known agonists and property matched decoys molecules. Finally, the same 3071 fragments that were screened experimentally were screened also by docking to the binding site of the α$_{2C}$ homology model using Glide. The modeled binding site is consequent with the mutagenesis and modeling data collected by Mátyus et al.[35] but with a more significant contribution to the site by the second extracellular loop. The top 1% (30 compounds) of the ranked ligand set went through the same hit validation protocol as described previously. 5 of the 30 compounds exhibited higher than 50% response in the cell-based α$_{2C}$ functional assay, but three of these also displayed higher than 30% fluorescence response at the sst$_4$ receptor. Finally, compounds **10** and **14** were identified from the virtual screening as validated hits preferring α$_{2C}$ binding. No false negatives of the primary experimental assay were identified. This ratio represents an enrichment factor of 12.8 (given that all actives were picked up by the primary assay in experimental screening) or less (if there were false negatives left unidentified). Docking and confirmation screening results are shown in Figure 2.

Binding modes of the hits feature the characteristic ionic H-bond with Asp131[3.32] and the protonated amine tails also form cation-π interactions with Phe423[7.39]. The aromatic or biaryl cores of the ligands are encased in a hydrophobic cage formed by
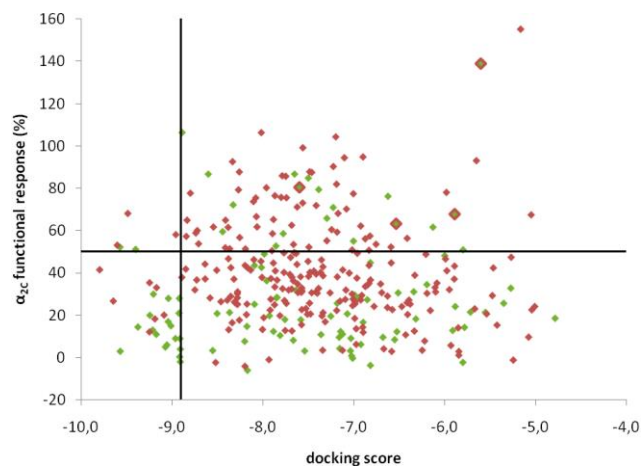
Figure 2. Docking scores vs. confirmation screening responses of the 318 fragments found active in primary screening and the 30 top ranking docked fragments. Green markers indicate <30% sst₄ response, red markers >30% sst₄ response, while framed markers indicate the four compounds inactive in the radioligand displacement assay.

Val132[3.33], Leu204[45.52], Ile211[5.39], Phe398[6.51] Phe399[6.52] and Tyr402[6.55]. Only compound **4** is capable of forming H-bonds with Ser214[5.42] and Ser218[5.46]. While these interactions were shown to be important in dopaminergic activation (compound **4** is also a known dopaminergic ligand), biphenyline- and clonidine-like agonists of alpha adrenergic receptors do not usually feature H-bonding moieties in this position. In our model an ion pair Arg192[45.40]-Asp206[45.54] from the second extracellular loop also protrudes in to form the binding site. While the arginine seems to be able to form cation-π interactions with aromatic moieties of biphenyline-like agonists and the hits identified in this study, no polar group in the ligands is seen to interact with this receptor feature. The predicted binding modes of the two agonists identified in virtual screening **10** and **14** are shown in Figure 3. Above the aforementioned interactions these ligands also feature a carbonyl group in a position suitable for forming an H-bond with the phenolic OH of Tyr402[6.55] and the tilt between the diaryl core allows a perfectly perpendicular arrangement of the tyrosine and the ligand aromatic planes. Structural information from modeling may also be used to rationally explore fragment modifications, however, this was out of the scope of this study.

2.3. Hit expansion

Following hit identification we progressed further to expand chemical space around hits. Different strategies are known for the development of active fragments[36] and in knowledge of ligand efficient modulators of α$_{2C}$ we attempted to optimize hits by scanning chemistry space while staying in the same size range. Therefore, our internal compound collection was searched for compounds with high structural similarity and comparable size to the selected hits, the latter expressed in heavy atom count. Up to five closest analogues for each hit with a K_i under 10 µM were picked from our compound library and tested for both functional and binding activity at 20 µM and if active, tested for affinity. This lower test concentration was a consequence of some of these fragment-sized compounds originating from the standard HTS screening library. From the tested compounds several possessed clearly improved binding affinity or ligand efficiency (see Table 2 for selected analogues of **17** and **10**) compared to the original parent structures, however all second round compounds tested in the functional assay turned out to act as antagonists of
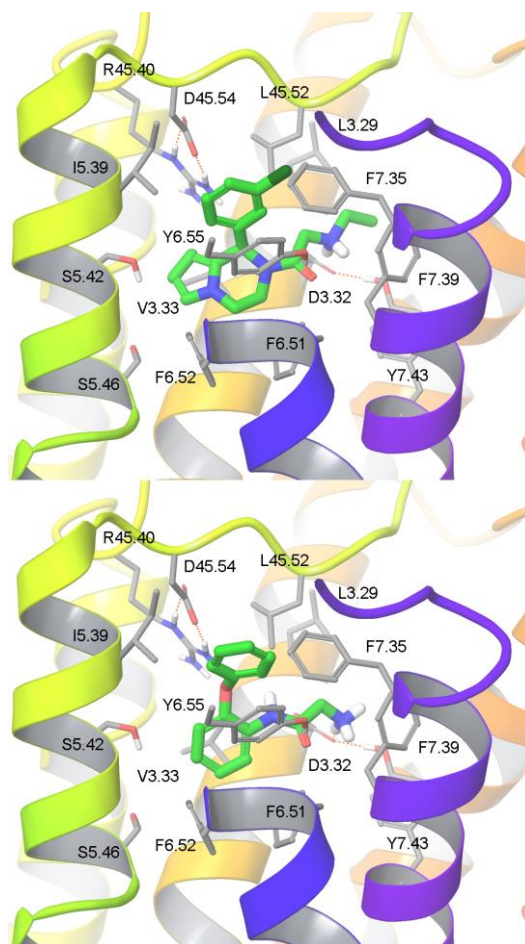

Figure 3. Predicted binding modes of the two agonists identified in virtual screening **10** (top) and **14** (bottom). Protein side chains are depicted in grey skeleton, ligands in green skeleton. The top of helix 6 is excluded for clarity.

the receptor, highlighting the high structural similarity of ligands with functionally opposing effects at α$_{2C}$. Hit expansion in this case was limited by availability of analogues in our compound collection, but in a more general setup it can be augmented from commercial sources and by targeted synthesis.

Table 2. Representative results of structural analogues of fragment hits in radioligand displacement and functional assays.

Cpd.	Structure	pKi	Inhibition %[a]	LE/LELP
18		6.25	-82	0.61 / 1.8
19		6.62	-87	0.65 / 1.7
20		4.86	N.D.	0.37 / 6.2

[a]Functional activity: Antagonism of responses elicited by 30 nM UK14,304 at 20 µM.

N.D. Not determined

3. Conclusions

Fragment screening has proven a viable approach for lead identification in drug discovery. Widely applied biophysical screening techniques provide efficient, though instrumentation intensive methods for various soluble protein targets, however their utility for some other major drug target classes like cell surface receptors and ion channels remains yet limited. Especially in the case of receptor agonists or potentiators, where stabilization of putative labile active conformations might be required, screening on a functional form of the targets could provide a viable alternative. In our study we have tested the utility of a conventional cell-based assay for high concentration screening of GPCR agonists and performed a head-to-head comparison with virtual screening by docking the same library to an active-like homology model of the α_{2C} adrenergic receptor. In addition to assessing the utility of the cell-based assay in primary screening we aimed at evaluation of a proposed screening workflow for the validation of fragment hits. Approximately 10% of the screened compounds were found active in our fragment screen for α_{2C} receptor agonists. This active rate, although much higher than under conventional HTS settings, is comparable to those reported for GPCRs using diverse assays as TINS, SPR,[10] intact cell binding[14] and conventional biochemical screening.[16,17] 24% of confirmed hits were found to prefer α_{2C} over an unrelated target, and 76% of these displayed significant activity in a biochemical assay as well. In virtual screening 2 out of the 16 hits were identified in the top 1% of the fragment library providing moderate enrichment but useful structural information on the hits. Our screening campaign successfully identified several potent and highly efficient chemotypes for α_{2C} agonists proving that conventional screening strategies could be successfully utilized in fragment-based lead discovery for membrane targets.

4. Experimental

4.1. Materials

UK14,304 and MK-912 and phentolamine were purchased from Sigma-Aldrich (St. Louis, MI). L-803,087 was obtained from Tocris Bioscience (Bristol, UK). Fragment collections were purchased from Maybridge (Cambridge, UK) and Albany Molecular Research Inc. (Albany, NY). Fragments were dissolved at 50 mM concentration in dimethyl sulfoxide (DMSO) and stored at -20 °C until use.

4.2. Structure-based virtual screening

The activated human adrenergic β_2 X-ray structures crystallized with the G protein complex (PDB ID: 3SN6) and with a stabilizing nanobody (PDB ID: 3P0G) were considered as templates for homology modeling of the adrenergic α_{2C} receptor. Side chain orientations in these two structural models are very similar but because of the fully resolved ECL2 loop, the latter structure was used as a template. The α_{2C} amino acid sequence (downloaded from UniProt, www.uniprot.org) was aligned with that of the structural template using Prime 3.2[37] after deletion of the nanobody. The sequence alignment is shown in the Supplementary information. Known agonists of the α_{2C} receptor in clinical and preclinical testing were downloaded from Thomson Reuters Integrity (integrity.thomson-pharma.com, accessed in July 2013) and prepared using LigPrep 2.6[38]. A single proto- and tautomer was generated at pH 7.4 by Epik 2.4[39]. These ligands were docked into the binding site of the homology model using the Induced Fit Docking (IFD) protocol in the Schrödinger Suite 2013.[40] Tyr127[3.28], Tyr402[6.55] and Phe423[7.39] side chains were truncated in the first round of the IFD protocol in order to

make space for the ligands and H-bonding with Asp131[3.32] was required in both the first docking and the redocking stages of the protocol.

Top ranking complexes from IFD were subjected to retrospective enrichment studies using 50 diverse actives from the Integrity ligand set and 2450 property matched (molar mass, formal charge, clogP and TPSA) decoys from vendor catalogs. Docking grids were centered on the reference ligand centroids and grid dimension was 10 Å for the inner and 24 Å for the outer box. Docking was performed using Glide 5.9[41] with and without H-bond constraints to Asp131[3.32]. 15 poses were included in post-docking minimization, otherwise settings were the default. The structure with the greatest area under the receiver-operating characteristic curve ($AUC_{ROC} = 0.720$) was used for docking the 3071 AMRI fragments in a prospective virtual screening setup. These were prepared similarly to the Integrity ligand set using LigPrep 2.6 and were docked similarly to the retrospective ligand set using Glide 5.9 without using the H-bond constraint to Asp131[3.32]. The top 1% (30 fragments) were included in hit validation protocols regardless of their primary experimental screening results in order to gain a full comparison of virtual and experimental screening. Docking scores were plotted against confirmatory experimental screening results and the maximal enrichment factor was calculated as ($n_{docking\ active}/n_{docking\ all}$)/($n_{screening\ active}/n_{screening\ all}$) = (2/30)/(16/3071) = 12.8. Similarity search was performed against our internal compound database as well as compounds having exact experimental data (i.e. inactives excluded) on the α_{2C} receptor in the ChEMBL database (www.ebi.ac.uk/chembl, accessed in August 2014) using the ChemAxon hashed linear fingerprint (fingerprint length = 1024, linear path length = 5, bits/path = 2) and Tanimoto similarity metric. Molecular properties (heavy atom count and clogP) were calculated using ChemAxon cxcalc 6.3.0.[42]

4.3. Cell culture and transfection

CHO-K1 cells stably expressing recombinant human α_{2C} adrenergic receptors and the chimeric $G\alpha_{qi5}$ protein were generated as described previously.[27] Cells were cultured in Ham's F12 nutrient mixture supplemented with L-glutamine (Gibco, Life Technologies, Carlsbad, CA) containing 10% foetal bovine serum (FBS, Gibco), 2.5 µg/ml amphotericin B, 100 U/ml penicillin G, 100 µg/ml streptomycin (Sigma), 1× non-essential amino acid mixture (Sigma), 1× RPMI-1640 vitamin solution (Sigma), 400 µg/ml G418 (Gibco), 200 µg/ml hygromycin (Invitrogen, Life Technologies, Carlsbad, CA).

CHO-K1 cells stably expressing recombinant human sst_4 receptors and $G_{\alpha16}$ were obtained from PerkinElmer (Waltham, MA) and were cultured in Ham's F12 containing 1× PSA (Sigma), 10% FBS, 400 µg/ml G418, 250 µg/ml zeocin (Invitrogen) according to the description provided by the supplier.

4.4. Membrane preparation from human α_{2C} expressing cells

Cells were cultured according to the instructions provided by the vendor. Harvested cell pellet was transferred into 10 vol. (w/v) of buffer A: 5 mM Tris, 5 mM EDTA, 0.2 mM EGTA, 1 mM phenylmethanesulfonylfluoride (PMSF), pH=7.5, at 22 °C and homogenized with Ultra-Turrax homogenizer (IKA, Staufen, Germany), at maximal speed for 15 sec. Cell homogenate was centrifuged at 30,000 g for 15 min at 4 °C. The resulting pellet was washed twice in homogenizing buffer and centrifuged at 30,000 g for 15 min at 4 °C. The final membrane pellet was resuspended in 3 vol (w/v) buffer B: 50 mM Tris, 1 mM EDTA, 5 mM MgCl$_2$, 1 mM PMSF, pH= 7.4, 22 °C. Protein content was

determined and membrane homogenate was diluted in buffer B to give a total protein concentration of 1 mg/ml. This final membrane homogenate was aliquoted and stored at -70 °C until use.

4.5. In vitro [^{3}H]UK14,304 binding assay

After thawing the aliquoted membrane homogenate in required quantity (40 μg total protein for each reaction) was diluted to a volume of 160 μl in buffer C: Tris 50 mM, pH=7.4, at 22 °C. Radioligand was diluted in buffer C to a volume of 20 μl [^{3}H]UK,14,304 (2 nM, specific activity 54 Ci/mmol, PerkinElmer), in the presence or absence of drugs (in 20 μl buffer C) incubated in a total volume of 0.2 ml for 30 min at 22 °C. For non-specific binding 10 μM phentolamine was used. After incubation samples were filtered over UniFilter® GF/C™ using Filtermate Harvester (PerkinElmer) and washed with 5×1 ml buffer C. The plate was dried at 50 °C for an hour and 20 μl Microscint™20 (PerkinElmer) scintillation cocktail was added to each well. The plate was read in a Microbeta counter (PerkinElmer). The ligand displacement by the compounds was determined using a minimum of six concentrations in duplicate or triplicate, and experiments were repeated at least two times. The specific radioligand binding is defined as the difference between total binding and the non-specific binding determined in the presence of an excess of unlabelled ligand. IC_{50} values (i.e. concentration of compound giving 50% inhibition of specific binding) was calculated from concentration-displacement curves by sigmoidal fitting using Origin 6.0 software (OriginLab, Northampton, MA). K_i values (i.e. inhibition constants) were calculated using the Cheng-Prusoff equation: $K_i = IC_{50}/[1+([L]/K_D)]$, where [L] is the radioligand concentration and K_D the affinity of the labelled ligand for receptor. K_D was determined from the Scatchard plot.

4.6. Fluorometric measurements

Fluorometric measurements of cytoplasmic calcium concentration ($[Ca^{2+}]_i$) were carried out in $\alpha_{2C}/G\alpha_{qi5}$ expressing cells and also in $sst_4/G_{\alpha 16}$ expressing cells. Cells were plated in standard tissue culture-treated 96-well microplates (40,000 cells/well) and maintained overnight in a tissue culture incubator at 37 °C under an atmosphere of 5% CO_2. Next day cells were loaded with 100 μl/well Ca^{2+}-sensitive dye FLIPR Calcium 4 (Molecular Devices, Sunnyvale, CA) for 45-60 min at 37 °C. Baseline and compound-evoked $[Ca^{2+}]_i$-changes were monitored with a plate reader fluorometer (FlexStation II[96], Molecular Devices) at 37 °C. The dye was excited at 485 nm and emission was sampled at 525 nm at 1.4-s intervals. After monitoring baseline fluorescence for 20 s, 50 μl/well agonist/compound solution, was added online using the pipettor of FlexStation, and fluorescence was recorded for an additional 40 s). Raw fluorescence data were transformed to ΔF/F values (F was the resting fluorescence preceding compound application and ΔF was the increase in fluorescence at a given time). In the case of the agonist measurements results were normalized to the response evoked by a maximally effective concentration of the reference agonists, UK14,304 (α_{2C}, 1 μM) or L-803,087 (sst_4, 3 μM). In the case of the α_{2C} antagonist measurements, cells were pre-treated with compounds/vehicle for 15 min and inhibitory potency of compounds was expressed as percent inhibition of the control agonist response (30 nM UK14,304, corresponding to an appr. EC_{80} concentration). All experiments were performed at least two times, on different days.

4.7. Fragment screening

Prior to screening, compounds were transferred to 384-well plates and diluted to 750 μM with buffer D (140 mM NaCl, 5 mM KCl, 2 mM $CaCl_2$, 2 mM $MgCl_2$, 20 mM D-glucose, 10 mM HEPES, pH=7.4) using a Biomek NX automated pipettor (Beckman Coulter, Brea, CA). Fluorometric calcium measurement was performed according to the above protocol with slight modifications, on an automated system using 384-well plates. Cells (12 500 cells/well in 20 μl) were plated into 384-well tissue culture-treated black wall, clear bottom plates (BD Biosciences, Franklin Lakes, NJ) using a Multidrop 384 dispenser (Thermo Fisher Scientific, Waltham, MA). Next day, medium was replaced with buffer D using a BioTek ELx405CW automated plate washer and 20 μl/well Ca^{2+}-sensitive dye FLIPR Calcium 5 (Molecular Devices) was added subsequently using a Multidrop dipenser. Cells were incubated for 25 min at 37 °C, followed by compound addition and fluorescence measurement in a FLIPR Tetra imaging plate reader (Molecular Devices). Responses were calculated from ΔF/F values normalized to control wells for vehicle (DMSO) and reference agonist (3 μM UK-14,304 or 5 μM L-803,087 for α_{2C} and sst_4, respectively) and expressed as percentage of positive control effect. Z' and Z parameters were calculated as described by Zhang et al.,[28] the latter from partial controls (displaying 63% activity in average).

Acknowledgments

Supplementary Material

Sequence alignment of the human α_{2C} receptor and the human β_2 receptor used in homology modeling.

References and notes

1. Erlanson, D. A. *Top. Curr. Chem.* **2012**, *317*, 1-32.
2. Leach, A. R.; Hann, M. M.; Burrows, J. N.; Griffen, E. J. *Mol. Biosyst.* **2006**, *2*, 430-446.
3. Jhoti, H.; Cleasby, A.; Verdonk, M.; Williams, G. *Curr. Opin. Chem. Biol.* **2007**, *11*, 485-493.
4. Chilingaryan, Z.; Yin, Z.; Oakley, A. J. *Int. J. Mol. Sci.* **2012**, *13*, 12857-12879.
5. Perspicace, S.; Banner, D.; Benz, J.; Müller, F.; Schlatter, D.; Huber, W. *J. Biomol. Screen.* **2009**, *14*, 337-349.
6. Lo, M. C.; Aulabaugh, A.; Jin, G.; Cowling, R.; Bard, J.; Malamas, M. et al. *Anal. Biochem.* **2004**, *332*, 153-159.
7. Boettcher, A.; Ruedisser, S.; Erbel, P.; Vinzenz, D.; Schiering, N.; Hassiepen, U. et al. *J. Biomol. Screen.* **2010**, *15*, 1029-1041.
8. Swinney, D. C.; Anthony, J. *Nat. Rev. Drug. Discov.* **2011**, *10*, 507-519.
9. Murray, C.W.; Verdonk, M. L.; Rees, D. C. *Trends Pharmacol. Sci.* **2012**, *33*, 224-232.
10. Congreve, M.; Rich, R. L.; Myszka, D. G.; Figaroa, F.; Siegal, G.; Marshall, F. H. *Methods Enzymol.* **2011**, *493*, 115-136.
11. Seeger, C.; Christopeit, T.; Fuchs, K.; Grote, K.; Sieghart, W.; Danielson, U. H. *Biochem. Pharmacol.* **2012**, *84*, 341-351.
12. Christopher, J. A.; Brown, J.; Doré, A. S.; Errey, J. C.; Koglin, M.; Marshall, F. H. et al. *J. Med. Chem.* **2013**, *56*, 3446-3455.
13. Chen, D.; Errey, J. C.; Heitman, L. H.; Marshall, F. H.; Ijzerman, A. P.; Siegal, G. *ACS Chem. Biol.* **2012**, *7*, 2064-2073.
14. Stoddart, L. A.; Vernall, A. J.; Denman, J. L.; Briddon, S. J.; Kellam, B.; Hill, S. J. *Chem. Biol.* **2012**, *19*, 1105-1115.
15. Wolkenberg, S. E.; Zhao, Z.; Mulhearn, J. J.; Harrison, S. T.; Sanders, J. M.; Cato, M. J. et al. *Bioorg. Med. Chem. Lett.* **2011**, *21*, 2646-2649.

16. Albert, J. S.; Blomberg. N.; Breeze, A. L.; Brown, A. J.; Burrows, J. N.; Edwards, P. D. et al. *Curr. Top. Med. Chem.* **2007**, *7*, 1600-1609.
17. Verheij, M. H.; de Graaf, C.; de Kloe, G. E.; Nijmeijer, S.; Vischer, H. F.; Smits, R. A. et al. *Bioorg. Med. Chem. Lett.* **2011**, *21*, 5460-5464.
18. Kobilka, B. K. *Trends. Pharmacol. Sci.* **2011**, *32*, 213-218.
19. Rasmussen, S. G.; DeVree, B. T.; Zou, Y.; Kruse, A. C.; Chung, K. Y.; Kobilka, T. S. et al. *Nature* **2011**, 477, 549-555.
20. Dror, R. O.; Arlow, D. H.; Maragakis, P.; Mildorf, T. J.; Pan, A. C.; Xu, H. et al. *Proc. Natl. Acad. Sci. USA* **2011**, *108*, 18684-18689.
21. Kohlhoff, K. J.; Shukla, D.; Lawrenz, M.; Bowman, G. R.; Konerding, D. E.; Belov, D. et al. *Nat. Chem.* **2014**, 6, 15-21.
22. Fairbanks, C. A.; Stone, L. S.; Kitto, K. F.; Nguyen, H. O.; Posthumus, I. J.; Wilcox, G. L. *J. Pharmacol. Exp. Ther.* **2002**, *300*, 282-290.
23. Gyires, K.; Zádori, Z. S.; Török, T.; Mátyus, P. *Neurochem. Int.* **2009**, *55*, 447-453.
24. Beuming, T.; Sherman, W. *J. Chem. Inf. Model.* **2012**, *52*, 3263-3277.
25. Renault, N.; Laurent, X.; Farce, A.; El Bakali, J.; Mansouri, R.; Gervois, P. *Chem. Biol. Drug. Des.* **2013**, *81*, 442-454.
26. Isberg, V.; Balle, T.; Sander, T.; Jørgensen, F. S.; Gloriam, D. E. *J. Chem. Inf. Model.* **2011**, *51*, 315-325.
27. Kurkó, D.; Bekes, Z.; Gere, A.; Baki, A.; Boros, A.; Kolok, S. et al. *Neurochem. Int.* **2009**, *55*, 467-475.
28. Zhang, J. H.; Chung, T. D.; Oldenburg, K. R. *J. Biomol. Screen.* **1999**, *4*, 67-73.
29. Hopkins, A. L.; Groom, C. R.; Alex, A. *Drug Discov. Today* **2004**, *9*, 430-431.
30. Keserű, G. M.; Makara, G. M. *Nat. Rev. Drug Discov.* **2009**, *8*, 203-212.
31. van Der Lee, M. M.; Bras, M.; van Koppen, C. J.; Zaman, G. J. J *Biomol. Screen.* **2008**, *13*, 986-998.
32. Harrison, C.; Traynor, J. R. *Life Sci.* **2003**, *74*, 489-508.
33. Ferenczy, G. G.; Keserű, G. M. *J. Med. Chem.* **2013**, *56*, 2478-2486.
34. Hann, M. M.; Leach, A. R.; Harper, G. *J. Chem. Inf. Comput. Sci.* **2001**, *41*, 856-864.
35. Balogh, B.; Szilágyi, A.; Gyires, K.; Bylund, D. B.; Mátyus P. *Neurochem. Int.* **2009**, *55*, 355-361.
36. Orita, M.; Ohno, K.; Warizaya, M.; Amano, Y.; Niimi, T. *Methods Enzymol.* **2011**, *493*, 383-419.
37. Prime, version 3.2, Schrödinger LLC, New York, NY, 2013.
38. LigPrep, version 2.6, Schrödinger LLC, New York, NY, 2013.
39. Epik, version 2.4, Schrödinger LLC, New York, NY, 2013.
40. Schrödinger Suite 2013-1 Induced Fit Docking protocol, Glide version 5.9, Prime version 3.2, Schrödinger LLC, New York, NY, 2013.
41. Glide, version 5.9, Schrödinger LLC, New York, NY, 2013.
42. Calculator, Version 6.3.0, © ChemAxon Ltd, 1998-2014.